© Photos: DOI: 10.2516/ogst/2013139, IFPEN, X

Dossier

This paper is a part of the hereunder thematic dossier published in OGST Journal, Vol. 69, No. 1, pp. 3-188 and available online here

Cet article fait partie du dossier thématique ci-dessous publié dans la revue OGST, Vol. 69, n°1, pp. 3-188 et téléchargeable ici

DOSSIER Edited by/Sous la direction de : **C. Angelberger**

IFP Energies nouvelles International Conference / Les Rencontres Scientifiques d'IFP Energies nouvelles

LES4ICE 2012 - Large Eddy Simulation for Internal Combustion Engine Flows

LES4ICE 2012 - La simulation aux grandes échelles pour les écoulements dans les moteurs à combustion interne

Oil & Gas Science and Technology – Rev. IFP Energies nouvelles, Vol. 69 (2014), No. 1, pp. 3-188

3> Editorial

11> *Boundary Conditions and SGS Models for LES of Wall-Bounded Separated Flows: An Application to Engine-Like Geometries*
Conditions aux limites et modèles SGS pour les simulations LES d'écoulements séparés délimités par des parois : une application aux géométries de type moteur
F. Piscaglia, A. Montorfano, A. Onorati and F. Brusiani

29> *LES of Gas Exchange in IC Engines*
LES échanges gazeux pour moteurs à combustion interne
V. Mittal, S. Kang, E. Doran, D. Cook and H. Pitsch

41> *Evaluating Large-Eddy Simulation (LES) and High-Speed Particle Image Velocimetry (PIV) with Phase-Invariant Proper Orthogonal Decomposition (POD)*
Évaluation de données de simulation aux grandes échelles (LES) et de vélocimétrie par imagerie de particules (PIV) via une décomposition orthogonale aux valeurs propres invariante en phase (POD)
P. Abraham, K. Liu, D. Haworth, D. Reuss and V. Sick

61> *Large Eddy Simulation (LES) for IC Engine Flows*
Simulations des grandes échelles et écoulements dans les moteurs à combustion interne
T.-W. Kuo, X. Yang, V. Gopalakrishnan and Z. Chen

83> *Numerical Methods and Turbulence Modeling for LES of Piston Engines: Impact on Flow Motion and Combustion*
Méthodes numériques et modèles de turbulence pour la LES de moteurs à pistons : impact sur l'aérodynamique et la combustion
A. Misdariis, A. Robert, O. Vermorel, S. Richard and T. Poinsot

107> *Investigation of Boundary Condition and Field Distribution Effects on the Cycle-to-Cycle Variability of a Turbocharged GDI Engine Using LES*
Études des effets des conditions aux limites et de la distribution des champs sur la variabilité cycle-à-cycle dans un moteur GDI turbocompressé en utilisant la LES
S. Fontanesi, S. Paltrinieri, A. D'Adamo and S. Duranti

129> *Application of LES for Analysis of Unsteady Effects on Combustion Processes and Misfi res in DISI Engine*
Application de simulation aux grandes échelles pour l'analyse des effets instationnaires de combustion et d'allumage raté dans les moteurs DISI
D. Goryntsev, K. Nishad, A. Sadiki and J. Janicka

141> *Eulerian – Eulerian Large Eddy Simulations Applied to Non-Reactive Transient Diesel Sprays*
Évaluation de la méthode Euler – Euler pour la simulation aux grandes échelles de sprays Diesel instationnaires non-réactifs
A. Robert, L. Martinez, J. Tillou and S. Richard

155> *Large-Eddy Simulation of Diesel Spray Combustion with Exhaust Gas Recirculation*
Simulation aux grandes échelles de la combustion d'un spray Diesel pour différents taux d'EGR
J. Tillou, J.-B. Michel, C. Angelberger, C. Bekdemir and D. Veynante

167> *Modeling of EGR Mixing in an Engine Intake Manifold Using LES*
Modélisation du mélange de EGR dans la tubulure d'admission à l'aide de la technique de LES
A. Sakowitz, S. Reifarth, M. Mihaescu and L. Fuchs

177> *LES of the Exhaust Flow in a Heavy-Duty Engine*
LES de l'écoulement d'échappement dans un moteur de camion
O. Bodin, Y. Wang, M. Mihaescu and L. Fuchs

Oil & Gas Science and Technology – Rev. IFP Energies nouvelles, Vol. 69 (2014), No. 1, pp. 167-176

DOI: 10.2516/ogst/2013118

IFP Energies nouvelles International Conference
Rencontres Scientifiques d'IFP Energies nouvelles

LES4ICE 2012 - Large Eddy Simulation for Internal Combustion Engine Flows
LES4ICE 2012 - La simulation aux grandes échelles pour les écoulements dans les moteurs à combustion interne

Modeling of EGR Mixing in an Engine Intake Manifold Using LES

A. Sakowitz[1,2]*, S. Reifarth[3], M. Mihaescu[1,2] and L. Fuchs[1,2]

[1] *CCGEx, KTH Mechanics, Royal Institute of Technology, 10044 Stockholm - Sweden*
[2] *Linné FLOW Centre, KTH Mechanics, Royal Institute of Technology, 10044 Stockholm - Sweden*
[3] *CCGEx, KTH Machine Design, Royal Institute of Technology, 10044 Stockholm - Sweden*
e-mail: sakowitz@mech.kth.se - reifarth@kth.se - mihai@mech.kth.se - lf@mech.kth.se

* Corresponding author

Résumé — **Modélisation du mélange de EGR dans la tubulure d'admission à l'aide de la technique de LES** — Nous étudions le processus de mélange des gaz d'échappement avec l'air dans les moteurs à combustion interne. Dans ce but, une simulation des grandes échelles (LES, *Large Eddy Simulations*) de l'écoulement compressible dans la tubulure d'admission d'un moteur Diesel à grosse cylindrée comptant 6 cylindres est réalisée. Le taux de recirculation des gaz d'échappement (EGR, *Exhaust Gas Recirculation*) est considéré comme un scalaire passif. Les résultats obtenus sont validés à l'aide des mesures du taux de EGR effectuées sur un moteur avec une sonde de mesure de CO_2. Les conditions aux limites de l'écoulement pulsatoire sont déduites de simulations unidimensionnelles et de mesures de pression effectuées sur le moteur. La qualité du mélange est évaluée à partir de la répartition d'un cylindre à l'autre et des moyennes quadratiques spatiales calculées au niveau des sections de sortie. Différentes méthodes sont utilisées pour le calcul des quantités moyennées. Les résultats montrent que les évolutions spatiales et temporelles de EGR sont différentes d'un cylindre à l'autre. La distribution de EGR dans l'orifice d'entrée du cylindre n'est pas uniforme. Ces facteurs impliquent que les moyennes temporelles ne devraient pas être utilisées pour décrire l'évolution de la teneur en EGR. De plus, les pulsations de l'écoulement, au niveau de l'orifice d'entrée de EGR, ont une forte influence sur la distribution de EGR. En comparant les résultats de simulations LES avec les résultats expérimentaux, nous montrons que les simulations LES permettent une meilleure et plus approfondie compréhension du processus de mélange lors d'études de tels écoulements turbulents et pulsatoires.

Abstract — ***Modeling of EGR Mixing in an Engine Intake Manifold Using LES*** — *We investigate the mixing process of exhaust gases with fresh air in Internal Combustion Engines (ICE). For this purpose, the flow in an inlet manifold of a six-cylinder heavy-duty Diesel engine is computed using compressible Large Eddy Simulations (LES). The Exhaust Gas Recirculation (EGR) concentration is modeled as a passive scalar. The results are validated by on-engine measurements of the EGR concentration using CO_2-probes. The boundary conditions for the highly pulsating flow are taken partly from one-dimensional simulations, partly from pressure measurements on the engine. In order to assess the sensitivity to the boundary conditions, changes are applied to the base-line case. The mixing quality is evaluated in terms of cylinder-to-cylinder distribution and the spatial RMS over the outlet cross-sections. Different averaging techniques are applied. It was found that the temporal and spatial*

EGR distribution is different among the cylinders. The EGR distribution within the cylinder inlet is non-uniform. These factors imply that one should not use a time-averaged EGR value as indicator for the EGR content. Furthermore, it was found that the flow pulsations at the EGR inlet have a large influence on the EGR distribution. By comparing the LES results with measurements, it was shown that LES gives a better and deeper insight into the mixing in such turbulent, pulsating flow situations.

INTRODUCTION

Exhaust Gas Recirculation (EGR) is a technique commonly used in modern Internal Combustion Engines (ICE), particularly in Diesel engines. EGR reduces nitrogen oxide (NO_x) emissions by lowering the oxygen concentration of the combustion gases and thereby the peak combustion temperature. This is possible because oxidation of nitrogen occurs only at high temperatures [1]. Due to stringent emission legislation EGR rates of up to 50% are applied in modern engines [2]. However, the EGR rate is limited by the increase of particulate emissions at high EGR rates.

In order to achieve EGR, parts of the exhaust gases have to be recycled and to be mixed with the fresh intake air. Due to space restrictions in the engine compartment, the distance from the mixing point to the cylinder intakes is often too short in order to provide homogenous air/EGR mixtures. A non-uniform mixture (both among and inside the cylinders) can result in an increase of NO_x and particulate emission as compared to a fully homogenous mixture. This has been shown by on-engine measurements performed for example by Maiboom *et al.* [3] and Payri *et al.* [2].

The issue of EGR/Air mixing has been studied experimentally using Particle Image Velocimetry (PIV) and Planar Laser Induced Fluorescence (PLIF) by Wiliam and Dupont [4] in a generic test bench. It was concluded that a Venturi nozzle significantly improves the mixture quality, but also increases the pressure losses and that large cycle-to-cycle variations may occur. The latter implies that time or ensemble averages of the concentration are not sufficient for the characterization of the mixing process.

In a study of Siewert *et al.* [5], an intake manifold for a passenger car was improved in terms of EGR and air mixing, using both experimental and computational methods. It was shown that they can be used to complement each other.

Reynolds Averaged Navier Stokes (RANS) computations have been applied by Karthikeyan *et al.* [6] analyzing the impact on the mixing properties of different mixer geometries. A previous study by Sakowitz and Fuchs [7] has compared Unsteady RANS (URANS) calculations to Large Eddy Simulation (LES) data with generic boundary conditions. It was found that the smoothing effect of URANS does not support the analysis of cycle-to-cycle variation.

The current report aims on the investigation of EGR mixing by LES. Implicit LES is applied to the intake manifold of a commercial 6-cylinder heavy-duty Diesel engine (*Fig. 1*). Common for this type of geometry is the presence of pipe bends upstream of the mixing point resulting in complex flow fields. These flows are among other things characterized by the formation of so called Dean vortices that occur due to flow curvature [8]. Furthermore, the presence of engine pulsations gives highly unsteady flow, particularly close to EGR inlet. The mixing quality is quantified in terms of cylinder-to-cylinder variation and the spatial variation of the

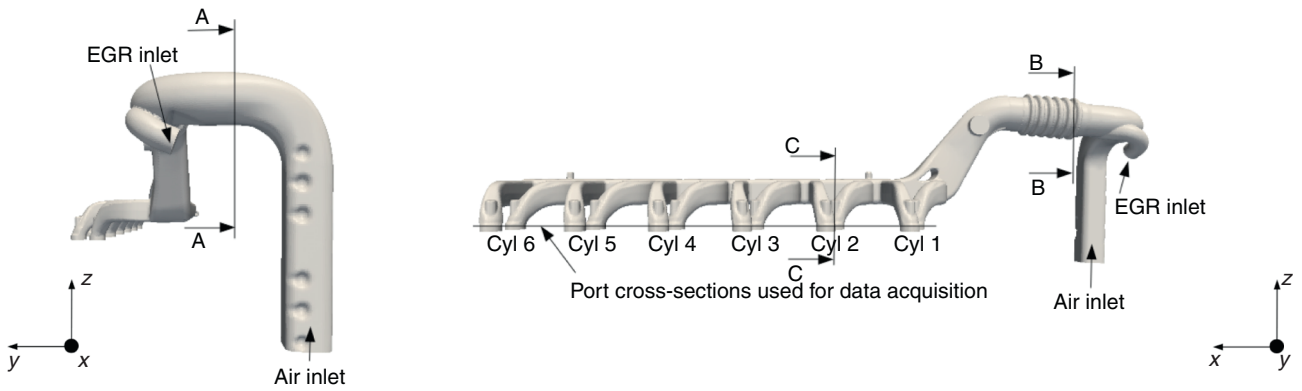

Figure 1

Inlet manifold from a Scania six cylinder Diesel engine including the definition of cross-sections used in the result section.

concentration. In order to validate the simulations, experiments were performed in close cooperation. Comparisons are done in terms of cycle-averaged EGR distribution.

A crucial issue of flow simulations in engines is the specification of realistic time-dependent boundary conditions. Most often they are estimated from one-dimensional tools. It is therefore important to assess the sensitivity to uncertainties in the boundary conditions. This is done by altering several parameters of the air and exhaust flow and the outflow to the cylinders.

1 METHODS

1.1 Large Eddy Simulation

The LES are based on the compressible Navier-Stokes equations, which can be written in the following form:

$$\frac{\partial \rho}{\partial t} + \frac{\partial}{\partial x_j}\left[\rho u_j\right] = 0 \tag{1}$$

$$\frac{\partial}{\partial t}(\rho u_i) + \frac{\partial}{\partial x_j}\left[\rho u_i u_j + p\delta_{ij} - \tau_{ij}\right] = 0 \tag{2}$$

$$\frac{\partial}{\partial t}(\rho e_0) + \frac{\partial}{\partial x_j}\left[\rho u_j e_0 + u_j p + q_j - u_i \tau_{ij}\right] = 0 \tag{3}$$

where ρ is the density, u_i is the velocity component in i-direction, e_o is the total energy defined as $e_o = e + \frac{1}{2}u^2$, e is the internal specific energy, p is the static pressure, τ_{ij} is the viscous stress tensor and q_i is the heat flux. In a Newtonian fluid, the viscous stresses are proportional to the strain rate. With the definition of the strain rate tensor:

$$S_{ij} = \frac{1}{2}\left(\frac{\partial u_i}{\partial x_j} + \frac{\partial u_j}{\partial x_i}\right) \tag{4}$$

τ_{ij} can be written as:

$$\tau_{ij} = 2\mu(S_{ij} - \frac{1}{3}S_{kk}\delta_{ij}) \tag{5}$$

Moreover, for the compressible form of the Navier-Stokes-equations, an equation of state is necessary in order to close the equation system. It is given by the ideal gas equation:

$$p = \rho R T \tag{6}$$

where R is the specific gas constant and T is the temperature.

In order to simulate the EGR concentration, an equation for a passive scalar is solved additionally. The equation describes passive transport of a mass fraction c by advection and molecular diffusion and has the following form:

$$\frac{\partial c}{\partial t} + u_i \frac{\partial c}{\partial x_i} = \frac{\partial}{\partial x_i}\left(D\frac{\partial c}{\partial x_i}\right) \tag{7}$$

where D is the molecular diffusivity. However, computing several scalars simultaneously with different diffusivities showed that the molecular diffusivity has only small effects on the mixture distribution in the present case and can be neglected. The mixing process is governed by the advective properties of turbulence and the flow pulsations.

LES resolves the large energy-carrying scales and models the small unresolved scales [9]. This is possible, because the smaller scales can be assumed to be universal and independent of the boundaries of the problem. In engine computations, the correct behavior of the small scales is not of interest but only their effect on the large scales. The main effect of the small scales are dissipation of turbulent kinetic energy. For large enough Reynolds numbers, the small scales, where dissipation is acting, are separated from the large scales by an inertial sub-range. According to Kolmogorov's theory this inertial sub-range is independent of viscosity. Under such conditions, the exact form of dissipation has no impact on the flow structures and on the large-scale end of the inertial sub-range. Thus, provided that the mesh resolution is fine enough (*i.e.* resolving a portion of the inertial sub-range whereby the dissipation effects are decoupled from the larger scales), the dissipative behavior, that is unavoidable when using second order schemes, can be used to model the unresolved scales instead of an explicit SGS (Sub-Grid Scale) model. This approach is called Implicit LES [10-13].

The described methods were implemented in the open source code OpenFoam using a pressure-based formulation and the Pressure Implicit with Splitting of Operators (PISO) algorithm for pressure-correction [14]. The maximum CFL number was held constant at 0.7.

1.2 Experiments

The experiments were carried out on a 13 liter six-cylinder heavy-duty Diesel engine with a power output of 360 hp.

To estimate the distribution of EGR in the intake manifold, the CO_2 concentration was measured in different locations. Two measurement probes at a time were placed inside the manifold, sucking the intake mixture to two gas analyzers. The probes were installed in flexible

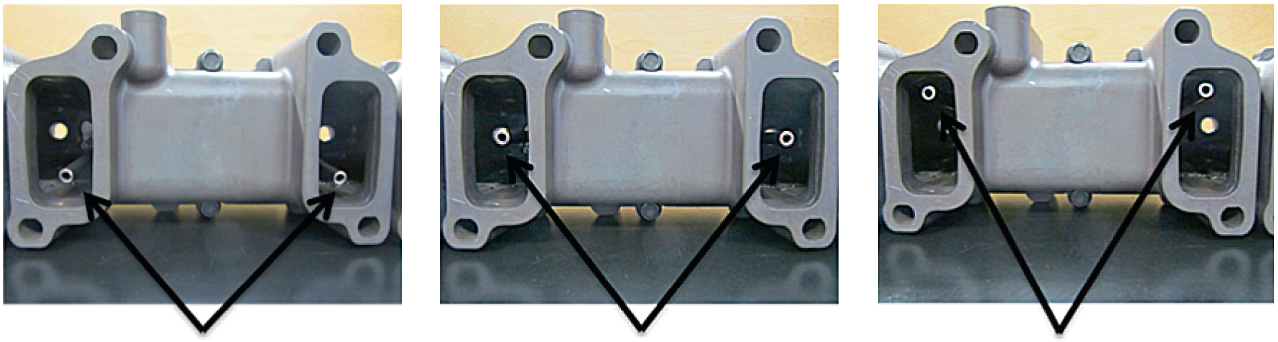

Figure 2

Measurement probes for the gas analyses.

ducts which allow to suck gas from different positions in the intake manifold. In each of the twelve ports, three positions were measured; bottom, center and top position, as visible in Figure 2. The measurement point lies in the plane that separates the intake manifold from the intake ducts.

For each measurement, the load point was set and run until all gas and coolant temperatures on the engine were stable. The CO_2-percentage was measured and averaged over 60 seconds. After the measurement, the engine was stopped to be able to move the probe position. All points were measured twice in random order to avoid the influence of drift of the measurement equipment. The trends were reproducible. The data presented in this article are averages over the three measurement positions for each port.

2 CONFIGURATION, MESH AND BOUNDARY CONDITIONS

The considered geometry for the simulations is the inlet manifold of the engine. EGR is introduced at a junction upstream of the cylinder ducts (*Fig. 1*). As it is common for engine manifolds, different pipe bends exist upstream of the EGR inlet.

The computational mesh is based on a precursor RANS-k-ε computation, from which the integral scales of the flow where estimated according to [15]. This lead to an estimation of a cell size of about 2-3 mm inside the domain and to about 1 mm close to walls. A hex-dominant mesh fulfilling these requirements was provided by Scania. The total amount of cells is about one million cells. In order to assure that this resolution gives adequate results, a comparison to a mesh resolution of 1-2 mm resulting in about 4 million cells was performed and showed only minor differences in terms of the EGR distribution.

To obtain the boundary conditions for the 3D-simulation, a combination of experiments and 1D-simulation was used. As inflow boundary conditions for the mesh, measured pressure traces from the air path and the EGR path of the engine were used. The outflow boundary condition, *e.g.* the mass flow, was computed from a calibrated 1D-simulation with the commercial software GT-Power. The considered load case is 1 200 rpm, the EGR rate is approximately 30% EGR.

Furthermore, the temperature was specified at the EGR and Air inlet according to one-dimensional simulations. The temperatures of the fresh air and the exhaust gases are fairly constant in time (within 3%).

Figure 3 shows the inlet and outlet conditions for one engine cycle. The resulting flow is highly pulsating with velocities at the EGR inlet ranging from −100 to 100 m/s. The Reynolds number based on the mean flow velocity and the largest diameter is about 500 000.

The boundary conditions for the EGR concentration is 1 at the EGR inlet, which corresponds to 100% EGR, and 0 at the air inlet. At the outlets a zero gradient condition is applied.

In order to assess the sensitivity to uncertainties in the boundary conditions, several changes are applied to this base-line case. The mass flow is specified as simplified triangular functions and the amplitude and temperature of the EGR pulses are changed.

The computational time was about 10 hours per engine cycle, when the process was distributed on 64 processors.

3 RESULTS

3.1 Description of the Flow Field

The piping upstream of the plenum consists of two 90-degree bends and one 45-degree bend. Additionally

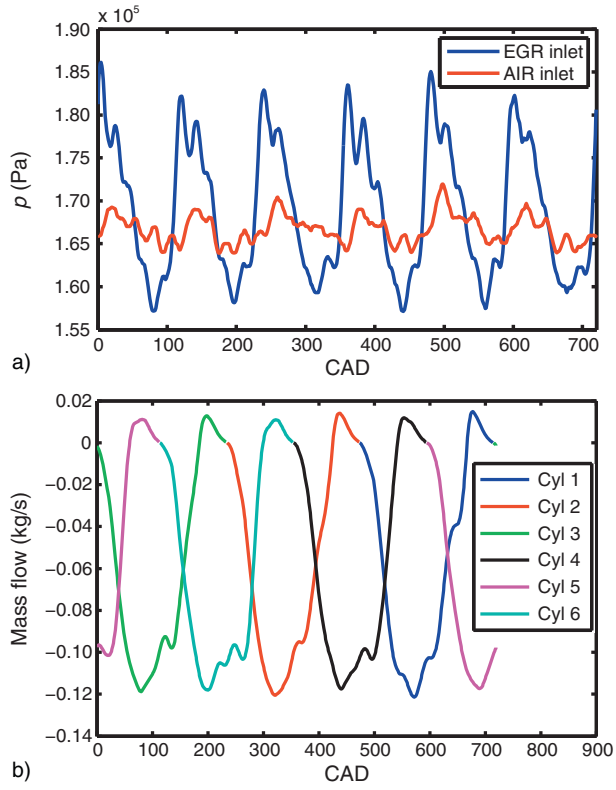

Figure 3

Boundary conditions; a) pressure from on-engine measurements, b) mass flow to cylinders from one-dimensional simulations.

to that the flow is strongly pulsating, particularly past the EGR inlet, which is situated at the second bend. Figures 4 and 5 show the inplane velocity vectors in cross-sections downstream of the first and the second bend at different phase angles (see *Fig. 1* for the position of the cross-sections). The background color in Figure 4 shows the magnitude of the streamwise velocity, whereas the background color in Figure 5 shows the phase-averaged EGR concentration. The data is phase-averaged over 20 engine cycles.

Dean vortices can be observed downstream of the first bend. However, the occurrence of these vortices depends on the pulsation phase. During the acceleration of the flow, the Dean-vortices are not yet established. They are developing at later times when the flow is at its maximum and are becoming stronger during the deceleration phase.

Past the second bend, the flow is governed by the EGR pulses coming in at the second bend. Due to the position of the EGR inlet pipe, the EGR flow is transported along the pipe walls and a counter-clockwise rotation is induced. This rotation is sustained throughout the plenum and is dominating the flow further downstream. This can be seen in Figure 6, which shows the strong rotation visible in the in-plane velocity vectors in cut C-C.

3.2 Mixture Distribution

The distribution of the exhaust gases among the cylinders and over the cylinder ports is evaluated at port cross-sections close to the outlets. For this purpose, the concentration, the velocity and the density were saved at the port cross-sections shown in Figure 1. The data was saved 100 times per engine cycle. Due to the low frequency response of the experimental apparatus, only time-averaged data over the whole cycle can be obtained experimentally. With LES, however, one is able to evaluate the percentage of EGR that actually passes a cross-section and goes into the cylinders by weighting the concentration with the mass flux through the ports. The conventional cycle average is given by:

$$c_{cycle\ average} = \frac{1}{NM}\sum_{i,j} c_{ij} \tag{8}$$

whereas the weighted average, which gives the EGR percentage of the flow into the cylinders, is defined by:

$$c_{into\ cylinder} = \frac{\iint c\rho u^n dAdt}{\iint \rho u^n dAdt} \approx \frac{\sum_{i,j} c_{ij}\rho_{ij}u^n_{ij}}{\sum_{i,j} \rho_{ij}u^n_{ij}} \tag{9}$$

Here, the index i denotes the time sample and the index j denotes the cell count over the cross-section. N is the number of samples and M the number of cells in the cross-section. u^n is the velocity normal to the considered cross-section and A is the cross-section area.

A measure for the mixing quality is the *spatial* Root Mean Square (RMS) of the concentration over the port cross-sections. Also the RMS can be weighted by the mass flux in order to exclude contributions from times where there is no flow through the port. The mean of the spatial RMS over a cross-section is computed as:

$$c_{rms\ cycle\ averaged} = \frac{1}{N}\sum_{i}\left(\sqrt{\frac{1}{(M-1)}\sum_{j}\left(c_{ij}-c_{i,mean}\right)^2}\right) \tag{10}$$

and the weighted RMS is defined as:

$$c_{rms\ into\ cylinder} = \frac{\sum_{i}\sqrt{\frac{1}{(M-1)}\sum_{j}\left[\rho_{ij}u^n_{ij}\left(c_{ij}-c_{i,mean}\right)\right]^2}}{\sum_{i,j}\rho_{ij}u^n_{ij}} \tag{11}$$

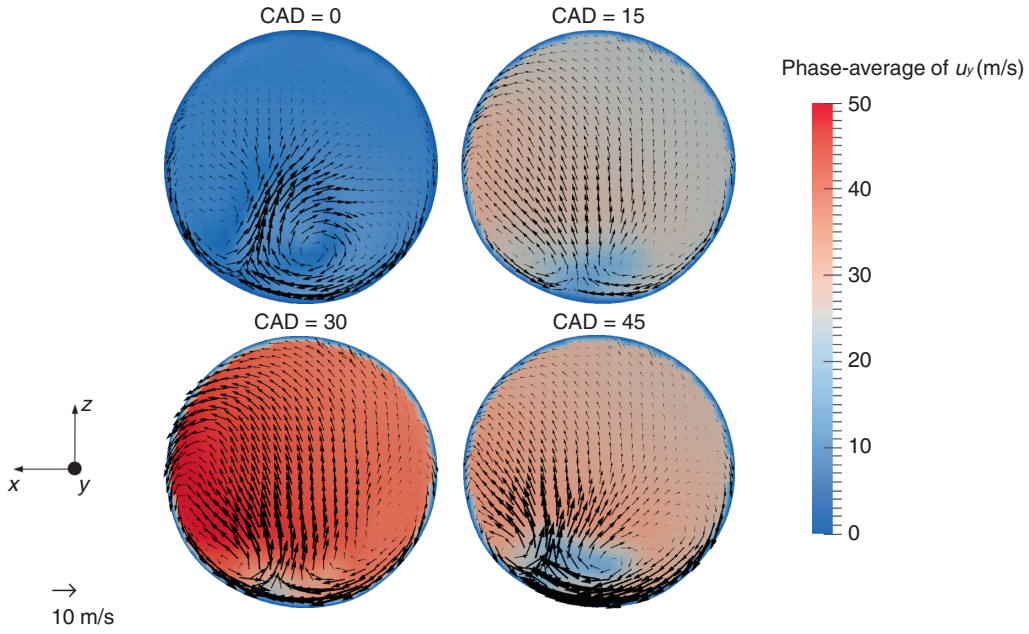

Figure 4

Phase averaged in-plane velocity vectors past the first bend (cut A-A) at different pulsation phases. Top left: minimum flow rate; top right: accelerating flow; bottom left: maximum flow rate; bottom right: decelerating flow; background color: phase-averaged velocity normal to the cross-section.

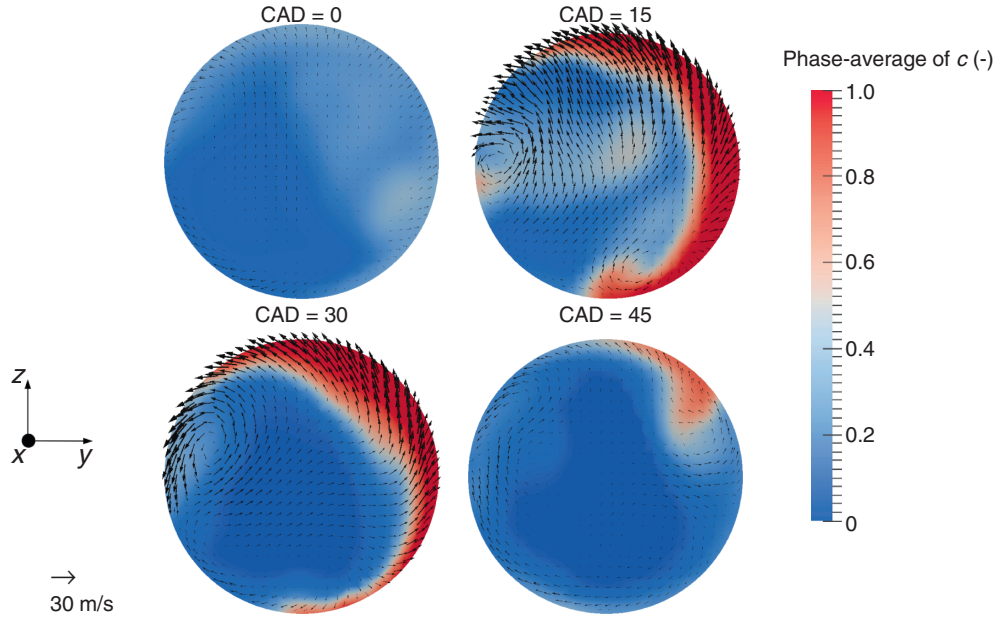

Figure 5

Phase averaged in-plane velocity vectors past the second bend (cut B-B) at different pulsation phases: Top left: minimum flow rate; top right: accelerating flow; bottom left: maximum flow rate; bottom right: decelerating flow; background color: phase-averaged EGR concentration.

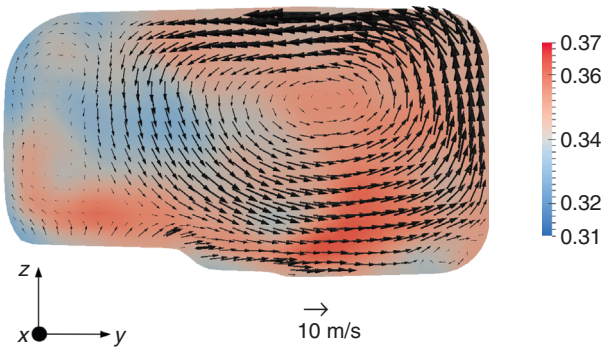

Figure 6

Phase-averaged in-plane velocity vectors at cut C-C at CAD = 200, *i.e.* flow through cylinder 6. Background color: phase-averaged EGR concentration.

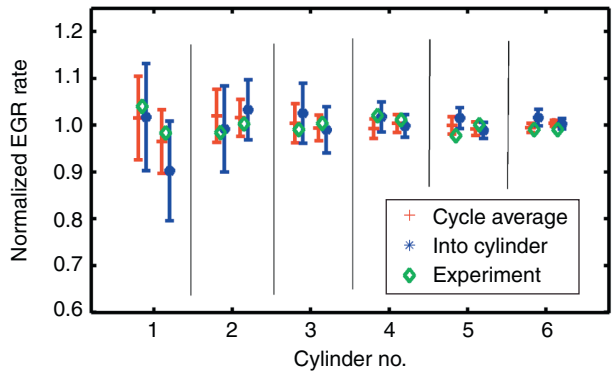

Figure 7

Different averages of cylinder-to-cylinder EGR distribution according to Equations (8) and (9). Bars indicate the spatial RMS of the concentration over the outlet cross-sections computed by Equations (10) and (11). The experimental data is the average of the three measurement points (*Fig. 2*).

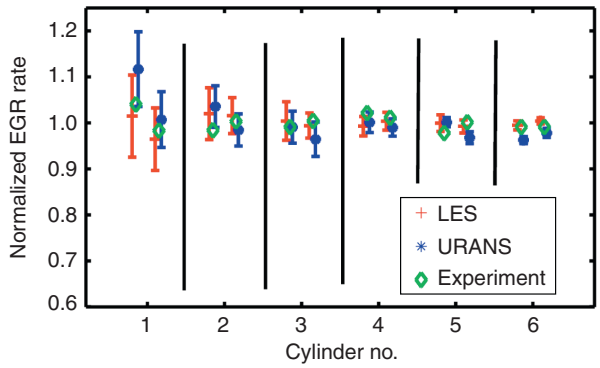

Figure 8

Comparison of LES cycle-averaged data with URANS results and experimental data.

where $c_{i,mean}$ is the mean of the concentration over the cross-section at time i.

All averages shown in the following paragraphs are averaged over at least 20 engine cycles, which corresponds to about 20 flow-through-times. 10 engine cycles were run before the data acquisition. The data are normalized with the mean EGR rate which changes slightly ($\pm 5\%$) depending on the inflow conditions.

Figure 7 shows the results for the base-line case. At the first cylinder, the spatial non-uniformity over the port cross-section is about 25%. Further downstream, the mixture quality is becoming better as can be seen by the decreasing RMS. The comparison with the experiments shows good agreement. The simulations and the experiments show the same trends and are within 5%.

It is evident from Figure 7 that large differences between the cycle average and the actual percentage of EGR flow to the cylinders can occur. At the second port of cylinder 1, the difference is about 8%. This result implies that the measurement of the time-average might be misleading. Furthermore, it can be concluded, that large non-uniformities over the cross-sections (up to 25%) can occur, even though the cycle average is close to unity.

In order to judge the benefits of LES over RANS, a comparison in terms of the cycle-averaged concentration and the spatial distribution over the cylinder ports between the precursor unsteady RANS-k-ϵ computation and the baseline LES is shown in Figure 8. Consistently with previous findings [7], unsteady RANS-k-ϵ overpredicts the non-uniformity among the cylinders by up to 10%. The reason is the non-physical smoothing effect of URANS which is not appropriate for accurate predictions of concentration distributions.

Figure 9 shows the phase-average of the concentration at a crank angle of 580 degrees, when the flow to cylinder 1 has its maximum value. The phase-average was performed on ten engine cycles. The EGR pulses can clearly be identified. At the time of flow into cylinder 1, there is a pulse of exhaust rich air directly in front of the first port. This is why the first port gets more EGR than the second one and implies that the EGR pulses are the major reason for the mal-distribution.

3.3 Sensitivity to Boundary Conditions

The sensitivity of the results to errors in the boundary conditions is assessed by introducing changes to the base-line case. One-dimensional tools, which are used for the estimation of boundary conditions, might be erroneous and the accuracy of these tools is hard to assess.

The sensitivity of the mixing process to the amplitude of the EGR pulses is analyzed by applying different EGR amplitudes. Figure 10 shows the different pressure boundary conditions.

The results in terms of the EGR distribution are shown in Figure 11. With increasing pressure amplitude, the cylinder-to-cylinder non-uniformity is increased. Also the RMS over the outlet ports is increased due to the introduction of larger pulsations. For the case of smaller pulsation amplitudes, the distribution is quite similar to the base line case. However, at the cylinders 4 to 6, an increase of the spatial RMS over the outlet ports as compared to the base line case can be observed. Pulsations are known to enhance mixing as compared to steady flow, which is the reason for the increased RMS with smaller pulsations. On the other hand, higher pulsations introduce larger non-uniformity in the flow, which explains the higher cylinder-to-cylinder variations with the larger pulsation amplitudes.

Figure 12 shows the EGR concentration with different temperature differences between the EGR temperature and the air temperature. Only slight differences can be seen in terms of cycle-to-cycle variation and the RMS over the cross-sections.

Finally, the sensitivity of the results to the outlet conditions is to be assessed. This is done using simplified outlet conditions. The mass flow to the cylinders is estimated as triangular functions (*Fig. 13*). An opening time of the valves of 200 CAD is assumed and the maximum mass flow is adjusted in order to achieve the same mass flow

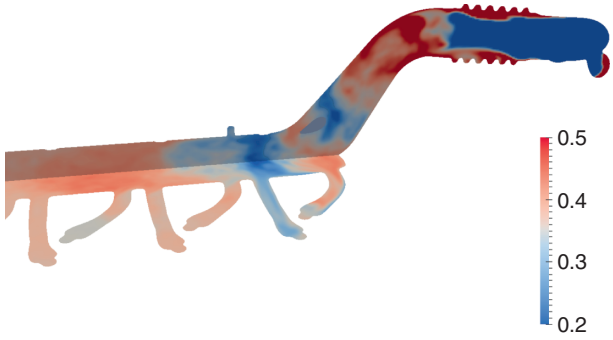

Figure 9

Phase average of the concentration at CAD = 580, *i.e.* maximum flow into cylinder one.

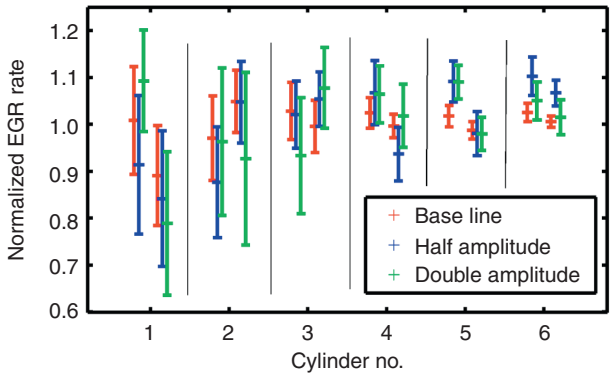

Figure 11

Normalized EGR Concentration $c_{into\ cylinder}$ (*Eq. 9*) for different EGR pressure pulse amplitudes. Bars indicate the RMS computed by Equation (11).

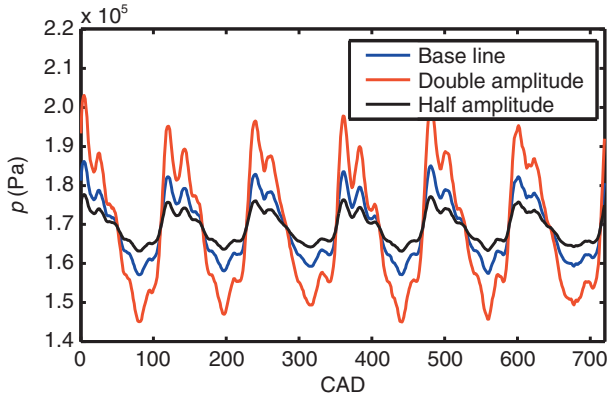

Figure 10

Pressure traces with different EGR inlet pressure amplitudes.

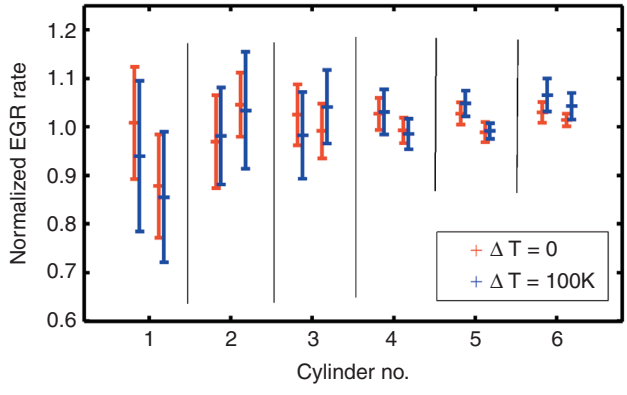

Figure 12

Normalized EGR Concentration $c_{into\ cylinder}$ (*Eq. 9*) for different temperature differences. Bars indicate the RMS computed by Equation (11).

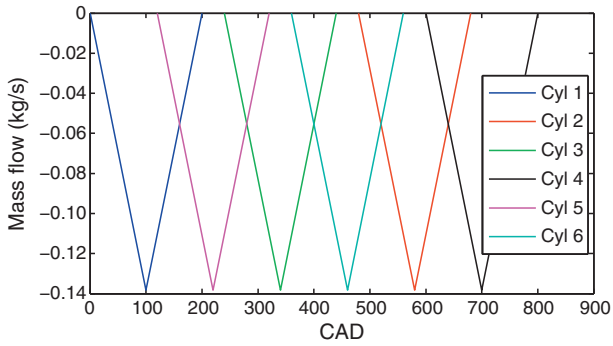

Figure 13

Simplified outlet boundary condition.

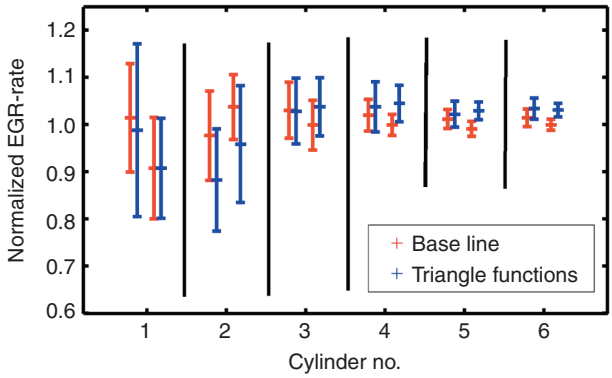

Figure 14

Normalized EGR Concentration $c_{into\ cylinder}$ (*Eq. 9*) for different outlet conditions. Bars indicate the RMS computed by Equation (11).

as with the GT Power data. The results are shown in Figure 14. There are significant deviations at cylinder 2. However, the general trends are unchanged.

4 CONCLUSIONS

The flow in an inlet manifold of a six-cylinder Diesel engine was analyzed using LES. The focus was the analysis of the mixing process between EGR and air. On-engine CO_2-measurements were performed in order to validate the results. The agreement between the experiments and the simulations was within 5%. It was shown that the EGR flow, which is highly pulsating, induces a flow rotation that is sustained throughout the plenum. The EGR pulsations were identified as the largest contributors to the non-uniformity. On the on hand, large pulsations are known to enhance mixing, on the other hand, large pulsations also introduce higher non-uniformity, which increases the cylinder-to-cylinder variation at the more upstream cylinders.

The LES results showed large deviations up to 20% over the port cross-sections. Moreover, different averaging methods indicated that simple time-averaging of the concentration might give misleading results, since it can significantly deviate from the EGR concentration of the actual flow into the cylinders.

A sensitivity study with respect to the boundary conditions was performed. The EGR concentration was found to be sensitive on the amplitude of the EGR pulsations. The temperature difference between the exhaust gases and the fresh air seemed to have little impact impact on the results. The same was found for a variation in the outlet conditions.

In summary, it was shown that LES is a suitable method to gain more understanding of the mechanisms governing the mixing process and gives important information on the flow not obtainable with the experimental methods. This implies that by LES one should be able to optimize the EGR distribution and thereby improve the engine's emission performance.

ACKNOWLEDGMENTS

The authors gratefully acknowledge the financial support by the Competence Center for Gas Exchange (CCGEx) and KTH. Scania's contribution in terms of providing the geometry and computational meshes is acknowledged. Computational resources were provided by HPC2N, Umeå university. Thanks also to Julie Vernet for translating the abstract to French.

REFERENCES

1 Heywood J.B. (1988) *Internal Combustion Engine Fundamentals*, McGraw-Hill, New York.

2 Payri F., Lujan J., Climent H., Pla B. (2010) Effects of the intake charge distribution in HSDI engines, SAE Technical Paper 2010-01-1119.

3 Maiboom A., Tauzia X., Hetet J.-F. (2009) Influence of EGR unequal distribution from cylinder to cylinder on NOx-PM trade off of a HSDI automotive Diesel engine, *Appl. Therm. Eng.* **29**, 2043-2050.

4 Wiliam J., Dupont A. (2003) Study of Geometrical Parameter Influence on Air/EGR Mixing, SAE Technical Paper 2003-01-1796.

5 Siewert R.M., Krieger R.B., Huebler M.S., Baruah P.C., Khalighi B., Wesslau M. (2001) Modifying an Intake Manifold to Improve Cylinder-to-Cylinder EGR Distribution in a DI Diesel Engine Using Combined CFD and Engine Experiments, SAE Technical Paper 2001-01-3685.

6 Karthikeyan S., Hariganesh R., Sathyanadan M., Krishnan S. (2011) Computational analysis of EGR mixing inside the intake system & experimental investigation on diesel engine for LCV, *Int. J. Eng. Sci. Tech.* **3**, 2050-2058.

7 Sakowitz A., Fuchs L. (2011) Computation of mixing processes related to EGR, *Proceedings of the 7th International Symposium on Turbulence and Shear Flow Phenomena*, Paper P38.

8 Dean W.R. (1928) The stream-line motion of a fluid in a curved pipe flow, *Philos. Mag.* **5**, 673.

9 Pope S.B. (2008) *Turbulent Flows*, Cambridge University Press.

10 Patnaik G., Boris J.P., Grinstein F., Fernando F. (2003) Large scale urban simulations with the MILES approach, *AIAA CFD Conference*, Orlando FL, 16th June 2003.

11 Grinstein F.F., Margolin L.G., Rider W.J. (2007) *Implicit Large Eddy Simulation: Computing Turbulent Fluid Dynamics*, Cambridge University Press, 23-26 June.

12 Garnier E., Adams N., Sagaut P. (2009) *Large Eddy Simulations for Compressible Flows*, Springer.

13 Aspden A., Nikiforakis N., Dalziel S., Bell J.B. (2008) Analysis of implicit LES Methods, *Comm. App. Math. and Comp. Sci.* **3**, 103-126.

14 Ferziger J.H., Peric M. (1996) *Computational Methods for Fluid Dynamics*, Springer.

15 Addad Y., Gaitonde U., Laurence D., Rolfo S. (2008) Optimal unstructured meshing for large eddy simulations. In Meyers J., Geurts B.J., Sagaut P. (eds), *Quality and Reliability of Large-Eddy Simulations in ERCOFTAC Series*, pp. 93-103, Springer Netherlands.

Manuscript accepted in February 2013
Published online in October 2013